Journal of Alloys and Compounds 506 (2010) 351–355

Contents lists available at ScienceDirect

Journal of Alloys and Compounds

journal homepage: www.elsevier.com/locate/jallcom

Growth of novel ZnO nanostructures by soft chemical routes

R. Saravana Kumar[a], R. Sathyamoorthy[a,*], P. Matheswaran[a], P. Sudhagar[b], Yong Soo Kang[b]

[a] PG and Research, Department of Physics, Kongunadu Arts and Science College (Autonomous), Coimbatore 641 029, Tamil Nadu, India
[b] Energy Materials Laboratory, WCU Program Department of Energy Engineering, Hanyang University, Seoul 133-791, South Korea

ARTICLE INFO

Article history:
Received 19 April 2010
Received in revised form 28 June 2010
Accepted 30 June 2010
Available online 13 July 2010

Keywords:
Nanostructured materials
Thin films
Semiconductors
Chemical synthesis
X-ray diffraction
SEM

ABSTRACT

We explore a facile route to prepare one-dimensional (1D) ZnO nanostructures including nanorods/nanospines on glass substrates by integrating inexpensive successive ionic layer adsorption and reaction (SILAR) and chemical bath deposition (CBD) methods. The effect of seed layer on the growth and morphology of the ZnO nanostructures was investigated. Accordingly, the surface modification of the seed layer prepared by SILAR was carried out by employing two different drying processes namely (a) allowing the hot substrate to cool for certain period of time before immersing in the ion-exchange bath, and (b) immediate immersion of the hot substrate into the ion-exchange bath. X-ray diffraction (XRD) analysis of the ZnO films revealed hexagonal wurtzite structure with preferential orientation along *c*-axis, while the scanning electron microscopy (SEM) revealed the dart-like and spherical shaped ZnO seed particles. ZnO nanostructures grown by CBD over the dart-like and spherical shaped ZnO seed particles resulted in the hierarchical and aligned ZnO nanospines/nanorods respectively. Room temperature photoluminescence (PL) study exhibited highly intense UV emission with weak visible emissions in the visible region. The growth mechanism and the role of seed layer morphology on the formation of ZnO nanostructures were discussed.

1. Introduction

For the past two decades, fabrication of novel nanostructures with different size and shapes has gained more attention, in particular 1D nanostructures have been extensively studied because of their potential applications in nanoelectronic devices such as field-effect transistors [1], single-electron transistors [2], photodiodes [3,4], and chemical sensors [5,6]. Zinc oxide (ZnO) with a wide direct band gap of 3.37 eV and large excitons binding energy of 60 meV at room temperature is considered as an excellent electronic and photonic material. The crystal size, orientation, surface area and morphology of the ZnO nanostructures play a vital role in some specific applications like sensors and catalysts [7]. ZnO nanostructures with different shapes and morphologies such as nanorods, nanodisks, nanowires, nanosheets, nanoneedles, nanoflowers have been demonstrated [8–11]. Among them, 1D ZnO nanorods with highly oriented and ordered arrays are considered essential for the development of novel nano-devices like UV lasers, solar cells, gas sensors, and varistors [12]. Generally, seed growth approach was extensively used to control the crystal growth behavior and orientation of ZnO. Prior seeding of the substrate by ZnO nanocrystals leads to the increase in the surface density of nucleation sites on which the ZnO nanorods can grow in a highly aligned fashion. A variety of chemical and physical deposition techniques like sputtering [13], sol–gel [14], pulsed laser deposition [15], spin coating [16] and thermal oxidation [17] have been employed to deposit the seed layer. However, these techniques often involve complex procedures, sophisticated equipments, or rigid experimental conditions and additional high-temperature annealing step which put serious limitation to the industrial applications. These limitations have stimulated research on the solution-phase synthesis (sometimes referred to as the soft solution route), which offers various advantages like low-cost, environmental benign, extensive control over nanostructure alignment and morphology and could be easily scaled-up to meet the industrial needs. An important and key issue is to grow ZnO nanorods, from aqueous solution at relatively low temperature (usually below 100 °C) which is both fundamentally interesting and technologically important. In addition, the solution growth technology is suitable to obtain stochimetrical ZnO films because of its oxygen-rich deposition environment, which may be beneficial for the suppression of deep levels related luminescence and the enhancement of UV emission. Among the several growth technologies, SILAR and CBD are the two charming methods widely used for growing nanostructured ZnO films. The mild reaction conditions, simple manipulation, easy control of the growth parameters, large-scale-up production and excellent material utilization efficiency have made these techniques as a good alternative for preparing nanostructured films. Yet the fabrication of different ZnO nanostructures through the soft chemical route in a rational way is

* Corresponding author. Tel.: +91 422 2642095; fax: +91 422 2644452.
E-mail addresses: rsathya59@gmail.com, saravanakumarak@yahoo.com (R. Sathyamoorthy).

0925-8388/$ – see front matter © 2010 Elsevier B.V. All rights reserved.
doi:10.1016/j.jallcom.2010.06.206

still a challenging task. Accordingly, in the present work we report a facile route to prepare 1D ZnO nanostructures through aqueous solution approach by combining both the SILAR and CBD technique. Fabrication of ZnO nanostructures with the aid of seed layer prepared by SILAR technique was seldom reported. The influence of the morphology of the seed layer on the growth and orientation of the ZnO nanorods was investigated, since the fundamental understanding of the effect of seed layer morphology is essential for the morphology and dimensionality-controlled growth of ZnO nanostructures for the efficient utilization in novel functional devices.

2. Experimental procedures

All the chemicals used in the present work were analytic grade and used without further purification.

2.1. Preparation of ZnO seed layer

ZnO seed layer was deposited by SILAR using aqueous zinc–ammonia complex as cation precursor and deionized water kept at 358 K as anionic precursor. The aqueous zinc–ammonia-complex ion ($[Zn(NH_3)_4]^{2+}$) was prepared by mixing zinc acetate dihydrate ($Zn(CH_3COO)_2{\cdot}2H_2O$) and ammonia ($NH_4OH$), with $Zn:NH_3$ molar ratio of 1:20 and Zn^{2+} concentration of 0.1 mol/L. The pH value of the resultant solution was 11. ZnO seed layer was deposited on glass substrate by alternate dipping in zinc ammonia complex and in hot water. In brief, each deposition cycle consists of four steps: (1) Immersion of the substrate in ($[Zn(NH_3)_4]^{2+}$) solution for 10 s for complex adsorption; (2) the instant immersion of the withdrawn substrates in hot water (358 K) for 12 s to form solid ZnO layer; (3) rinsing the substrate in deionized water to remove the unreacted species (4) drying the substrate in air for 30 s before the start of the next deposition cycle. Surface modification of the seed layers was carried out by altering the preparation conditions. The substrate was allowed to dry for 10 s during the substrate withdrawing process from the hot water. The films prepared by the application of drying process were named as D1, while the films prepared without drying process as D2. Typically, 40 deposition cycles (rather than 20 and 30 deposition cycles) were performed to probe the growth and orientation of the ZnO nanostructures.

2.2. Growth of ZnO nanostructures

The ZnO nanorods/nanospines were grown on the seed coated substrate using the bath containing $Zn(CH_3COO)_2{\cdot}2H_2O$, NH_4OH and triethanolamine (TEA) as a zinc source, a base and a stabilizer respectively. The aqueous zinc–ammonia-complex ion was prepared as mentioned above with same molar ratio and concentration. To this complex solution, 0.2 M of TEA was added and the mixture was stirred for few minutes before placing in the water bath. The deposition was carried at 353 K for 3 h.

2.3. Characterization

The structural and morphological properties of the ZnO films were examined by Bruker Axs D8 using X-ray diffractometer CuKα radiation (λ = 1.5406 Å) and JEOL JSM-6330F field emission scanning electron microscopy. The room temperature PL spectra were recorded using Xenon lamp with a wavelength of 325 nm as excitation source.

3. Growth mechanism of ZnO films

3.1. SILAR

The experimental process of SILAR involves the successive immersion of the substrate in cationic and anionic solutions and rinsing the substrate in the ion-exchange water in between. A thin layer of liquid film of the precursor ions is absorbed on the substrate first, and then the solid film is formed via the chemical reaction between the adsorbed ions and precursor ions with the opposite charge. Accordingly, in the present work, ZnO film was deposited on glass substrate by alternate dipping in $[Zn(NH_3)_4]^{2+}$ kept at room temperature and in hot water maintained at 358 K.

The $[Zn(NH_3)_4]^{2+}$ used for the deposition of ZnO seed layer was prepared by mixing NH_4OH (25% ammonia solution) and aqueous $Zn(CH_3COO)_2{\cdot}2H_2O$ solution. Initially white precipitate appears due to the formation of $Zn(OH)_2$, which dissolves on further addition of NH_4OH, thus forming $[Zn(NH_3)_4]^{2+}$ complex. The overall reaction leading to the formation of $[Zn(NH_3)_4]^{2+}$ complex is given by

$$Zn(OH)_2 + 4NH_4OH \rightarrow [Zn(NH_3)_4]^{2+} + 2OH^- + 4H_2O \quad (1)$$

During the reaction period in hot water, $[Zn(NH_3)_4]^{2+}$ complex first decomposes to $Zn(OH)_2$ precipitate and then subsequently transforms to ZnO. The transformation of $Zn(OH)_2$ to ZnO occurs at temperatures beyond 323 K [18]. The reaction occurring on the surface of the substrate leading to the formation of ZnO is given by

$$[Zn(NH_3)_4]^{2+} + H_2O \rightarrow Zn(OH)_2 + 4NH_4{}^+ + 2OH^- \rightarrow ZnO_{(S)} + H_2O \quad (2)$$

The ZnO crystal formed will serve as nuclei for further film growth.

3.2. CBD

It is well known that in CBD technique the formation of oxide film is a result of competence between heterogeneous nucleation (on the surface of the substrates) and homogenous nucleation (in the bulk of the solutions). The principle of this process is based on the solubility product and ionic product, where the film formation

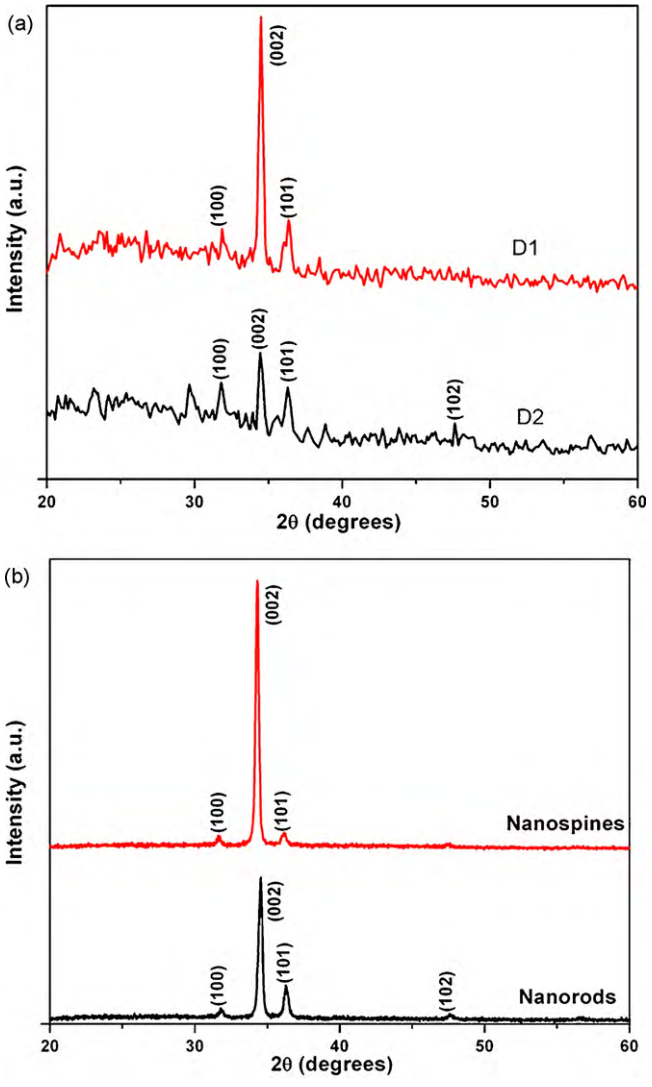

Fig. 1. XRD pattern of (a) ZnO seed layer and (b) ZnO nanostructured film deposited on the seeded substrate.

on the substrate takes place when the ionic product exceeds the solubility product by heterogeneous nucleation onto the substrate. To avoid the homogenous nucleation, molar ratio of the complexing agent to the zinc source and pH of the solution should be maintained appropriately. Accordingly, in the present work, the molar ratio of Zn:NH_3 was kept at 1:20 and the pH of the solution is maintained at 10.5.

Typical assembly of ZnO nanostructures on the seeded substrates is as follows; initially white precipitate appears when NH_4OH was added to the aqueous solution of $Zn(CH_3COO)_2{\cdot}2H_2O$ due to the formation of $Zn(OH)_2$. However, on further addition of ammonia, the precipitates dissolve completely forming ($[Zn(NH_3)_4]^{2+}$) complex.

$$Zn(CH_3COO)_2 + 2NH_4OH \rightarrow Zn(OH)_2 + 2NH_4COOCH_3 \quad (3)$$

$$Zn(OH)_2 + 4NH_4OH \rightarrow [Zn(NH_3)_4]^{2+} + 2OH^- + 4H_2O \quad (4)$$

Addition of TEA replaces the amine to form complex ion $[Zn(N(C_2H_4OH)_3)_4]^{2+}$:

$$[Zn(NH_3)_4]^{2+} + N(C_2H_4OH)_3 \rightarrow [Zn(N(C_2H_4OH)_3)_4]^{2+} + 4NH_3 \quad (5)$$

When the solution is heated at 353 K, dissociation of the complex ions on the glass substrates takes place to form ZnO.

$$[Zn(N(C_2H_4OH)_3)_4]^{2+} \rightarrow ZnO + NH_3 + H_2O + CO_2 \quad (6)$$

The physical adhesion of the ZnO nanostructures was tested and it showed good mechanical stability against peeling.

4. Results and discussion

Fig. 1a shows the XRD pattern of samples D1 and D2 deposited on glass substrates by SILAR. All the peaks in the XRD pattern could be indexed to hexagonal wurtzite structure of ZnO, which are good agreement with the standard card (JCPDS 36-1451). No diffraction peaks of the impurities such as $Zn(OH)_2$ or zinc acetate was detected in both the cases, indicating the high purity and single phase nature of the obtained film. ZnO films prepared by D2 exhibited weak crystallinity and typical polycrystalline nature, whereas a strong preferential orientation along (0 0 2) plane was observed for the films prepared by D1. Drying process just after the reaction in hot water is very imperative for the crystallization process of ZnO films. The rapid evaporation of water from the ZnO layer and the heat treatment in the hot air flux coming from the hot surface will maintain long-range order structure of the ZnO particles, forming highly crystalline structure [19]. The mean crystallite sizes of the ZnO films were determined using the (0 0 2) peak and the Debye–Scherrer's equation [20] given by:

$$D = \frac{k\lambda}{\beta \cos\theta} \quad (7)$$

where, the constant 'K' is the shape factor = 0.94, 'λ' the wavelength of X-rays (1.5406 nm for CuKα), 'θ' is the Bragg's angle and 'β' is the half width of diffraction peak measured in radians. The mean crystallite sizes of the samples D1 and D2 were found to be 25 nm and 21 nm respectively.

Fig. 1b shows the XRD patterns of ZnO nanostructured films grown on ZnO seed coated substrates (D1 and D2). The diffraction intensity of the (0 0 2) peak is much stronger than that of the other peaks such as (1 0 0) and (1 0 1), indicating that the ZnO crystals grow preferentially perpendicular to the substrate surface i.e. c-axis oriented growth. The lattice parameters were calculated using the observed values of 2θ and d-values for the hexagonal structure. The lattice constant of the nanostructured ZnO films deposited on D1 were a = 3.259 Å, c = 5.224 Å; while for the films deposited on D2 were a = 3.246 Å, c = 5.208 Å. The measured c/a axial ratio of 1.603 and 1.604 for the films deposited on D1 and D2 respectively, showed a good match with the value of 1.602 for the ideally close packed hexagonal structure [21].

Fig. 2a and c shows the SEM images of the ZnO seed layer samples D1 and D2 respectively. Sample D1 exhibited sub-micron

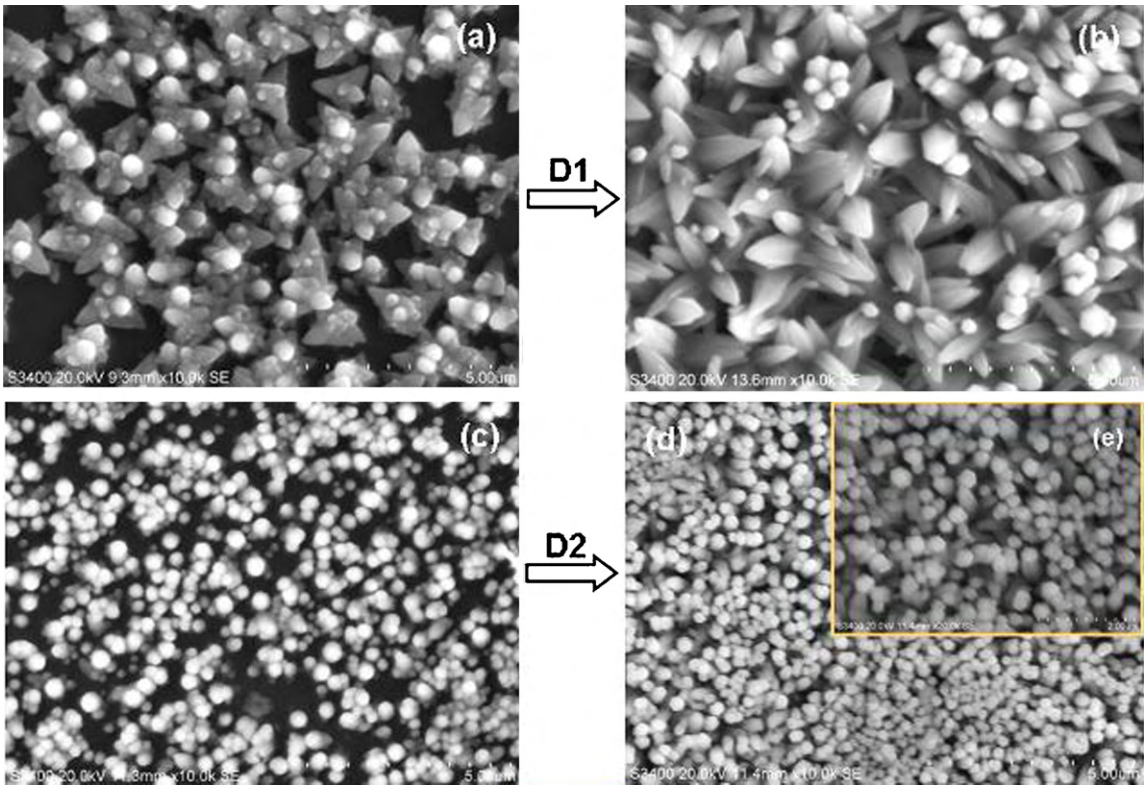

Fig. 2. SEM image of (a) and (c) ZnO seed layer; (b) and (d) ZnO nanospines/nanorods grown on the seeded substrate; (e) higher magnification image of the ZnO nanorods.

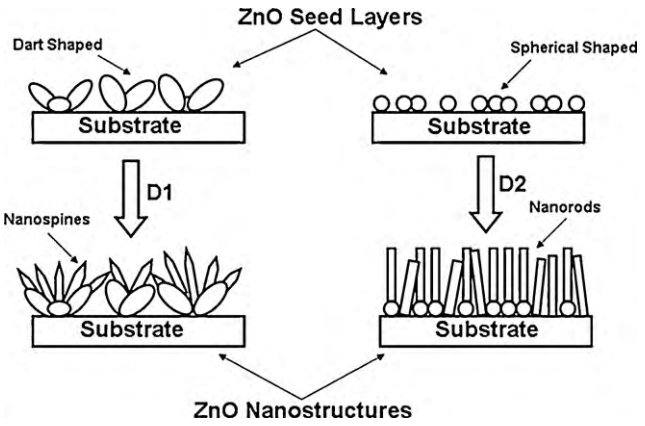

Fig. 3. Growth mechanisms of ZnO nanorods/nanospines.

sized elongated semi-ellipsoid particles combined to form dart-like structures and further the sub-micron sized particles are made by the aggregation of smaller ZnO crystallites. On the other hand, sample D2 show spherical shaped ZnO particles made of interfused smaller crystallites such that no clear boundary between the neighboring crystallite can be observed. Sudden quenching (without the application of drying process) in the ion-exchange water results in the removal of weakly bonded ZnO particles on the surface of the growing film, whereas the drying process helps in improving the effective adsorption of the ions on the growing films. Heating at elevated temperature and subsequently applying the drying process transforms the loosely attached congeries to dense sub-micron particle with the semi-ellipsoid shape.

Fig. 2b and d shows the SEM images of the hierarchical and aligned ZnO nanospines/nanorods grown on the seed coated substrates D1 and D2 respectively. The high density of the nucleation sites on the surface of the seed layer facilitates the growth of nanostructures and the morphology of the underlying seed layer plays an important role for the growth and orientation of the nanostructures. The dart-like morphology of D1 resulted in the hierarchical growth of ZnO nanospines, whereas the spherical surface morphology of D2 leads to the growth of vertically aligned ZnO nanorods. The inset 2(e) shows the higher magnification image of the hexagonal shaped ZnO nanorods.

On the basis of the above experimental observations, the growth mechanism of hierarchical and aligned ZnO nanospines/nanorods is depicted as shown in Fig. 3. The seed layer is imperative for the growth of high-quality ZnO nanostructures, since the size of the nanoparticles on the substrate determines the size of the growing ZnO nanostructures. The presence of seed layer effectively lowers the nucleation energy barrier and cause heterogeneous nucleation to occur easily. When the nanoparticles are applied as the seeds, nanocrystal orientation and alignment could be accomplished through competition [22]. Since the seeds are not well aligned to the substrate surface, the ZnO crystals grew along the fastest growth orientation without any alignment initially. However, as the randomly oriented rod-like crystals grew further, they began to overlap and their growth became physically limited as the misaligned nanorods began to impinge on other neighboring crystals, giving rise to the preferred orientation of the film.

In SILAR process, experimental parameters like zinc precursor, molar ratio of Zn:NH_3, pH, drying process and reaction time in hot water influences the growth and crystallization behavior of the ZnO films. Nevertheless, the rinsing process used to remove the loosely absorbed particles also has considerable impact on the deposition process and film quality. In addition, the microstructure and the crystalline quality of the ZnO films can be modified by replacing the conventional mechanical rinsing with ultrasonic rinsing.

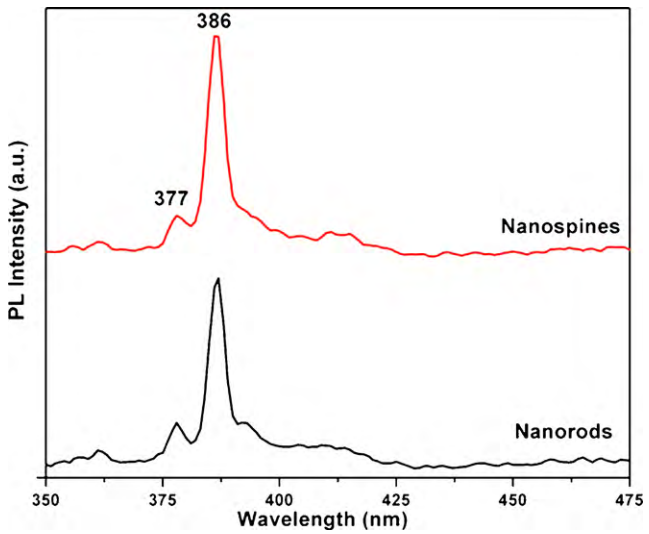

Fig. 4. PL spectra of ZnO nanorods/nanospines.

The extreme conditions (transient temperature up to ~5000 K, pressure up to 1800 atm., and cooling rate in excess of 1011 K/s) induced by the acoustic cavitations generates active nucleation sites on the surface of the particles, thereby creating materials with novel structures and unusual properties like smaller size and higher surface area [23]. The influence of ultrasonic irradiation on the morphology and the subsequent ZnO nanostructure growth are under investigation.

The optical properties of the ZnO nanostructures were investigated by PL measurements. Fig. 4 shows the room temperature PL spectra of the ZnO nanostructured films deposited on D1 and D2 respectively. Normally, ZnO nanostructures exhibit UV emission and visible emission. The UV emission is attributed to the near-band edge emission of ZnO due to the annihilation of excitons [24], while the visible luminescence mainly originates from the surface defect states such as Zn interstitials and oxygen vacancies [25]. One of the key issues on ZnO photoluminescence is the suppression of defect emission either by varying the preparation conditions or post-fabrication treatments [26]. In the present case, the PL spectra of ZnO nanorods/nanospines exhibit strong near-band edge UV emission at ~377 nm and 386 nm, and relatively very weak visible emission in blue band (410–450 nm). The good crystalline quality of the seed layer (D1) and the corresponding ZnO nanospines resulted in enhanced PL intensity than that of the ZnO nanorods. Nevertheless, the high intensity ratio of the UV emission to defect emission indicates the good crystallization of the ZnO nanostructures.

5. Conclusions

ZnO nanorods/nanospines were successfully prepared by integrating the novel soft chemical routes namely SILAR and CBD technique. Experimental results showed that the selection of seed layers is very crucial for obtaining highly ordered and good quality ZnO nanostructures. The growth and orientation of the ZnO nanostructures was tailored by tuning the morphology of the seed layer. Accordingly, the spherical shaped and dart-like morphology of the ZnO seed layers resulted in the growth of ZnO nanorods and nanospines respectively. The films possessed good crystal quality and exhibited strong UV emission. The high optical quality of the ZnO nanostructures presented here, are very prospective for their applications in optoelectronic nanodevices, such as light-emitting diodes, UV lasers, dye sensitized solar cells and field-effect transistors. Furthermore, the soft chemical routes employed could speed

up the preparation of high-quality ZnO nanostructures and the strategy presented here is expected to prepare other transition metal oxide nanomaterials.

Acknowledgements

One of the authors R. Sathyamoorthy gratefully acknowledges Department of Science and Technology (DST), New Delhi for this work supported through DST/CMP-50 project. Two of the authors (P. Sudhagar and Yong Soo Kang) acknowledge Engineering Research Center program through the National Research Foundation of Korea (NRF) grant funded by the Ministry of Education, Science and Technology (MEST) (No. 2009-0063369) and also by Future-based Technology Development Program (Nano Fields) through the NRF funded by the MEST (No. 2009-0082843).

References

[1] S.-W. Chung, J.-Y. Yu, J.R. Heath, Appl. Phys. Lett. 76 (2000) 2068–2070.
[2] A. Notargiacomo, L. Di Gaspare, G. Scappucci, G. Mariottini, E. Giovine, R. Leoni, F. Evangelisti, Mater. Sci. Eng. C 23 (2003) 671–673.
[3] O. Hayden, R. Agarwal, C.M. Lieber, Nat. Mater. 5 (2006) 352–356.
[4] P. Feng, J.Y. Zhang, Q.H. Li, T.H. Wang, Appl. Phys. Lett. 88 (2006) 153107.
[5] C. Li, D. Zhang, X. Liu, S. Han, T. Tang, J. Han, C. Zhou, Appl. Phys. Lett. 82 (2003) 1613–1615.
[6] A. Kolmakov, Y. Zhang, G. Cheng, M. Moskovits, Adv. Mater. 15 (2003) 997–1000.
[7] X. Liu, Z. Jin, S. Bu, J. Zhao, Z. Liu, J. Am. Ceram. Soc. 89 (2006) 1226–1231.
[8] T. Long, S. Yin, K. Takabatake, P. Zhnag, T. Sato, Nanoscale Res. Lett. 4 (2009) 247–253.
[9] I. Levin, A. Davydov, B. Nikoobakht, N. Sanford, P. Mogilevsky, Appl. Phys. Lett. 87 (2005) 103110.
[10] H. Sun, M. Luo, W. Weng, K. Cheng, P. Du, G. Shen, G. Han, Nanotechnology 19 (2008) 125603.
[11] U.N. Maiti, Sk.F. Ahmed, M.K. Mitra, K.K. Chattopadhyay, Mater. Res. Bull. 44 (2009) 134–139.
[12] B. Cao, X. Teng, S.H. Heo, Y. Li, S.O. Cho, G. Li, W. Cai, J. Phys. Chem. C 111 (2007) 2470–2476.
[13] Q. Li, J. Bian, J. Sun, J. Wang, Y. Luo, K. Sun, D. Yu, Appl. Surf. Sci. 256 (2010) 1698–1702.
[14] S.-H. Hu, Y.-C. Chen, C.-C. Hwang, C.-H. Peng, D.-C. Gong, J. Alloy Compd. 500 (2010) L17–L21.
[15] C. Zhang, J. Phys. Chem. Solids 71 (2010) 364–369.
[16] X. Hu, Y. Masuda, T. Ohji, K. Kato, Thin Solid Films 518 (2009) 906–910.
[17] Z. Lockman, Y.P. Fong, T.W. Kian, K. Ibrahim, K.A. Razak, J. Alloy Compd. 493 (2010) 699–706.
[18] T. Pauporte, D. Lincot, Electrochic. Acta 45 (2000) 3345–3353.
[19] X.D. Gao, X.M. Li, W.D. Yu, Thin Solid Films 484 (2005) 160–164.
[20] P.K. Baviskar, W. Tan, J. Zhang, B.R. Sankapal, J. Phys. D: Appl. Phys. 42 (2009) 125108.
[21] S.-C. Liou, C.-S. Hsiao, S.-Y. Chen, J. Cryst. Growth 274 (2005) 438–446.
[22] Z.R. Tian, J.A. Voigt, J. Liu, B. Mckenzie, M.J. Mcdermoott, R.T. Cygan, L.J. Criscenti, Nat. Mater. 2 (2003) 821–826.
[23] X.D. Gao, X.M. Li, W.D. Yu, Appl. Surf. Sci. 229 (2004) 275–281.
[24] X. Qu, D. Jia, Mater. Lett. 63 (2009) 412–414.
[25] H. Li, M. Xia, G. Dai, H. Yu, Q. Zhang, A. Pan, T. Wang, Y. Wang, B. Zou, J. Phys. Chem. C 112 (2008) 17546–17553.
[26] A.B. Djurisic, Y.H. Leung, Small 2 (2006) 944–961.